

# Topographical organization of pathways from somatosensory cortex through the pontine nuclei to tactile regions of the rat cerebellar hemispheres

Trygve B. Leergaard,<sup>1</sup> Sveinung Lillehaug,<sup>1</sup> Erik De Schutter,<sup>2</sup> James M. Bower<sup>3</sup> and Jan G. Bjaalie<sup>1</sup>

<sup>1</sup>Centre for Molecular Biology and Neuroscience & Institute of Basic Medical Sciences, University of Oslo, Oslo, Norway

<sup>2</sup>Theoretical Neurobiology, Department of Biomedical Sciences, University of Antwerp, Antwerp, Belgium

<sup>3</sup>Research Imaging Center, University of Texas Health Science Center at San Antonio, San Antonio, TX, USA

**Keywords:** 3-D reconstruction, axonal tracing, brain maps, cerebellum, corticopontine pathways, pontocerebellar pathways

## Abstract

The granule cell layer of the cerebellar hemispheres contains a patchy and noncontinuous map of the body surface, consisting of a complex mosaic of multiple perioral tactile representations. Previous physiological studies have shown that cerebrocerebellar mossy fibre projections, conveyed through the pontine nuclei, are mapped in registration with peripheral tactile projections to the cerebellum. In contrast to the fractured cerebellar map, the primary somatosensory cortex (SI) is somatotopically organized. To understand better the map transformation occurring in cerebrocerebellar pathways, we injected axonal tracers in electrophysiologically defined locations in Sprague–Dawley rat folium crus IIa, and mapped the distribution of retrogradely labelled neurons within the pontine nuclei using three-dimensional (3-D) reconstructions. Tracer injections within the large central upper lip patch in crus IIa-labelled neurons located centrally in the pontine nuclei, primarily contralateral to the injected side. Larger injections (covering multiple crus IIa perioral representations) resulted in labelling extending only slightly beyond this region, with a higher density and more ipsilaterally labelled neurons. Combined axonal tracer injections in upper lip representations in SI and crus IIa, revealed a close spatial correspondence between the cerebropontine terminal fields and the crus IIa projecting neurons. Finally, comparisons with previously published three-dimensional distributions of pontine neurons labelled following tracer injections in face receiving regions in the paramedian lobule (downloaded from <http://www.rbwb.org>) revealed similar correspondence. The present data support the coherent topographical organization of cerebro-ponto-cerebellar networks previously suggested from physiological studies. We discuss the present findings in the context of transformations from cerebral somatotopic to cerebellar fractured tactile representations.

## Introduction

The granule cell layer of the cerebellar cortex receives direct somatosensory inputs from numerous brain stem nuclei and the spinal cord. The tactile mossy fibers subserve a discontinuous ‘fractured’ map in the hemispheres of the rat cerebellum (Shambes *et al.*, 1978; Bower *et al.*, 1981; Bower & Kassel, 1990; Shumway *et al.*, 1999; Hartmann & Bower, 2001). This has been studied in particular detail in the rat cerebellar folium crus IIa, which contains representations of perioral and intraoral regions, such as the upper lip, lower lip, incisors, and vibrissae. These representations are found at multiple locations throughout the folium, with new neighbouring relationships occurring in each location (reviewed in Welker, 1987; Voogd, 1995; Fig. 1C).

While direct afferent sensory projections provide considerable mossy fibre input to the cerebellar granule cell layer, the largest source of mossy fibers arises from the pontine nuclei, which in turn are innervated by massive projections from the cerebral cortex (Brodal, 1972). Previous physiological studies have demonstrated that electrical stimulation of specific body part representations in the primary somatosensory cortex (SI) and tactile stimulation of corresponding

body surfaces activate closely matching parts of the cerebellar granule cell layer (Bower *et al.*, 1981; Morissette & Bower, 1996), thus indicating that SI-ponto-cerebellar projections are aligned with the fractured pattern of primary afferent projections. The fact that tactile surfaces are somatotopically represented in a continuous map in SI (Woolsey & Van der Loos, 1970; Welker, 1971; Chapin & Lin, 1984; Fabri & Burton, 1991; Fig. 1A) implies that a map transformation must occur somewhere in the SI-ponto-cerebellar pathway. The present experiments continue our efforts to understand the detailed anatomical structure of this important pathway, as well as to determine where the transformation from a somatotopic to a fractured map takes place.

The three-dimensional (3-D) topography of the SI-pontine projection, the first link in this pathway, has been documented in detail (Leergaard *et al.*, 2000a, b, 2004). Each body part representation in SI is typically projected onto two or three locations in the pontine nuclei. Among these axonal clusters, the neighbouring relationships of the SI somatotopic map are largely preserved, albeit with a potential for introduction of new neighbouring relationships (reviewed in Leergaard, 2003; Fig. 1B). Thus, the transformation into multiple discontinuous representations in the cerebellar granule cell layer cannot be fully explained from the organization of cerebropontine projections.

We have investigated the distribution of pontocerebellar neurons in relation to corresponding cerebro-pontine projections. Axonal tracers

Correspondence: Dr Jan G. Bjaalie, as above.

E-mail: j.g.bjaalie@medisin.uio.no

Received 2 April 2006, revised 28 August 2006, accepted 30 August 2006

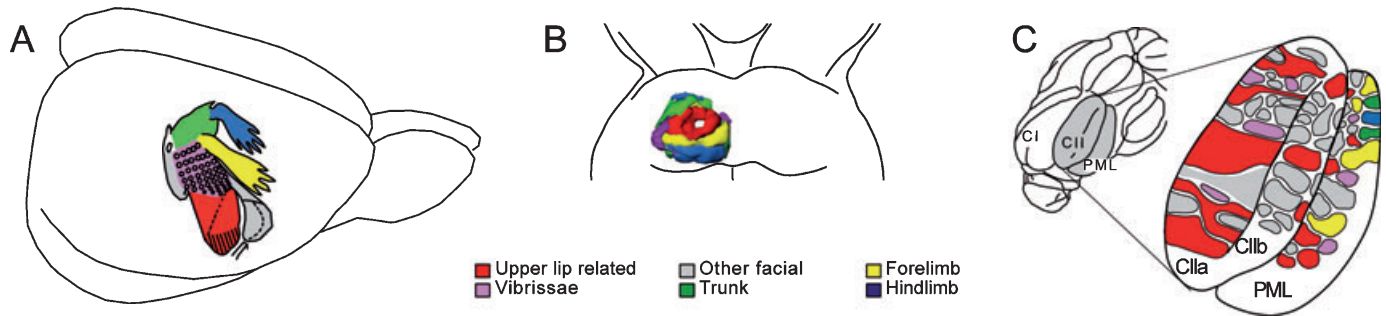


FIG. 1. Map transformations in the somatosensory system. Tactile information from the body surface is somatotopically mapped in the primary somatosensory cortex (A). This essentially two-dimensional (2-D) cortical map is transformed into a more complex 3-D map in the pontine nuclei (B), in which somatotopic relations are largely preserved. In the granule cell layer of the cerebellar hemispheres, somatosensory representations are organized in a more complex and disrupted map, referred to as a fractured map, as here shown in crus IIa and the PML (C). Modified from Bjaalie & Leergaard (2005).

were either applied to a single patch in crus IIa (one perioral body representation) or to multiple patches (multiple perioral body representations) in crus IIa. The distributions of retrogradely labelled pontine neurons were 3-D reconstructed, transferred to a standardized coordinate system, and compared to previously obtained maps of SI pontine projections (Leergaard *et al.*, 2000b) and pontine projections to other parts of the cerebellum (Odeh *et al.*, 2005; see also, Pijpers & Ruigrok, 2006). In addition, dual injections in SI and crus IIa were used to validate some of these comparisons.

## Materials and methods

### Surgical procedures

A total of 15 adult female Sprague–Dawley rats (Simonsen Laboratories, Gilroy, CA, USA; Scanbur BK AS, Nittedal, Norway) were used. All animal procedures were approved by an institutional animal welfare committee (at the California Institute of Technology and at the University of Oslo) and were in compliance with national laws in both countries, and in particular with the US National Institutes of Health guidelines for the use and care of laboratory animals. The animals were anaesthetized with intramuscular injection of 0.20–0.25 mL/kg of a mixture of ketamine hydrochloride (25%, 100 mg/mL), xylazine (6.3%, 20 mg/mL), and acepromazine maleate (0.25%, 10 mg/mL), followed by an intraperitoneal injection of sodium pentobarbital

(50 mg/mL; 0.05–0.06 mL/kg). Supplementary injections of the drug mixtures (one-third) were given every 2 h after the first injection. Two of the animals were not submitted to electrophysiological mapping. These animals were anaesthetized by subcutaneous injection of 3 mL/kg of a mixture of equal volumes of Hypnorm (fentanyl citrate 0.315 mg/mL and fluanisone 10 mg/mL, Janssen, High Wycombe, UK) and Dormicum (midazolam 5 mg/mL, Hoffmann-La Roche, Basel, Switzerland). During surgery, animals were placed on a heating pad with rectal temperature feedback to maintain stable body temperature. The head was positioned and immobilized in a stereotaxic frame, the cerebellar and/or cerebral cortex exposed, and the dura removed.

### Electrophysiological mapping in crus IIa and SI

Prior to axonal tracer injections, micromapping was performed in the cerebellar and/or cerebral cortex.

In crus IIa, the aim was to identify the large, centrally located, ipsilateral upper lip patch at the crown of the folium (Figs 1C and 2A and B). A digital image of the exposed area was recorded. The micromapping techniques used in these experiments are described in detail elsewhere (Bower & Kassel, 1990). In short, a tungsten electrode connected to an amplifier and a loudspeaker set-up, was slowly advanced into the crus IIa perpendicularly to the cerebellar surface and into the granular cell layer. The surface of the animal was

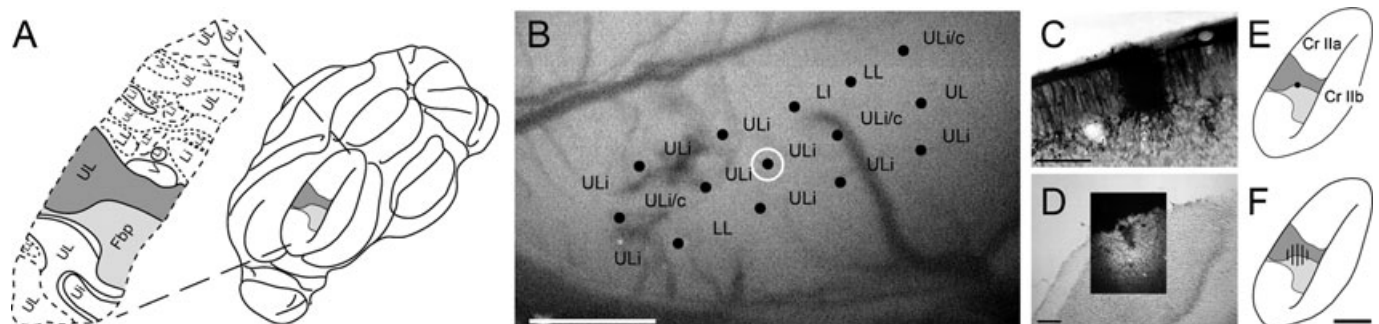


FIG. 2. Electrophysiological mapping of tactile representations and neuronal tracer injections in crus IIa. (A) Illustration showing the location of the cerebellar crus IIa, and the pattern of fractured somatotopic organization of tactile representations in the crown of crus IIa (modified from Bower & Kassel, 1990). The large centrally located upper lip related patch is indicated by shades of grey. (B) Example videoimage of the exposed left crus IIa. Electrode recording positions are indicated by black dots. Small amounts of axonal tracer were deposited centrally in the electrophysiologically identified large centrally located upper lip related representation, at position indicated by white open circle. (C) Microscope image of transverse sections through the cerebellar cortex showing an example small BDA injection site. (D) Composite image showing a slightly larger Fluoro-Gold injection site in a fluorescence microscopy image view (small frame) superimposed on a light microscope view of crus IIa. (E–F) Simplified diagram of Crus IIa in which the size and extent of the injection sites are indicated. LI, lower lip; UL, upper lip; ULi, ipsilateral upper lip; ULc, contralateral upper lip; V, vibrissae. Scale bars, 500  $\mu$ m (B); 150  $\mu$ m (C and D), and 1000  $\mu$ m (E and F).

then gently tapped and stroked until audible responses were heard. Maximal multiunit responses were found in the granule cell layer, ranging from 400 to 800  $\mu\text{m}$  deep to the pial surface. The exact recording position of each electrode penetration was registered on the brain surface image together with information about the body part(s) that generated the response. The mapping sequence consisted of three lines of punctures running along the mediolateral axis of the folium. For most experiments recording sites along these lines were separated by 150  $\mu\text{m}$  or less. These procedures have previously been shown to be sufficient to accurately identify patch boundaries of the larger patches (Gonzalez *et al.*, 1993).

In the SI cortex, similar procedures were used to identify the upper lip or perioral representations electrophysiologically (see Leergaard *et al.*, 2000b concerning details regarding surgery and electrophysiological mapping of these animals).

### Tracer injections

Following the electrophysiological mapping, different axonal tracers were either deposited in the centre of the large upper lip related patch at the crown of crus IIa, or distributed across the entire crown of crus IIa, covering multiple perioral representations. In SI, tracers were applied to the centre of the upper lip representation. In the two animals not submitted to electrophysiological mapping, anatomical and molecular criteria were used for placing the tracer inside the large, centrally located, ipsilateral upper lip related patch at the crown of crus IIa. The interindividual variations of the boundaries of this patch at the crown of crus IIa were sufficiently small (Bower & Kassel, 1990) to allow an experienced operator to place an injection based on stereotaxic coordinates, visually identified vascular patterns, and distance from the midline. The correct location was verified by staining every second section through the cerebellar injection site with monoclonal antibodies raised against zebrin II (Hawkes & Leclerc, 1986) and mapping the tracer location in relation to the available maps on the correspondence between zebrin patterns and electrophysiologically defined representations (Hallem *et al.*, 1999).

Several axonal tracers and methods of tracer delivery were used. In brief, solutions of 2.5% wheat germ agglutinin-horseradish peroxidase (WGA-HRP; Sigma, St. Louis, MO, USA), 10% biotinylated dextran amine (BDA; Molecular Probes, Eugene, OR, USA), and 2.5% *Phaseolus vulgaris*-leucoagglutinin (Pha-I; Vector Laboratories, Burlingame, CA, USA), were injected iontophoretically through a glass micropipette. Solutions of 2.0% fluoro-gold (FG; Fluorochrome Inc., Englewood, CO, USA) and 10% rhodamine conjugated dextran amine (FluoroRuby, FR, Molecular Probes, Eugene, OR, USA) were pressure injected using a glass micropipette cemented to the tip of a 1- $\mu\text{L}$  Hamilton syringe, placed in a microinjection unit (Kopf 5000, Kopf Instruments, Tujunga, CA, USA). Finally, crystals of FR were implanted using the method described by Glover (1995).

### Histochemistry

After survival periods of 3 days (WGA-HRP injected cases) or seven days (all other cases), the animals were re-anaesthetized with an overdose of sodium pentobarbital (50 mg/kg *i.p.*) and perfused transcardially with lukewarm physiological saline, lukewarm fixative and finally cold 10% sucrose. All solutions were prepared in 0.1 M phosphate buffer. As fixative, the WGA-HRP injected animals received a mixture of 1% paraformaldehyde and 1.25% glutaraldehyde, whereas the remaining animals received 4% paraformaldehyde. The brains were removed, photographed and stored in 30% sucrose for 1–5 days prior to sectioning.

All sections were cut at 50  $\mu\text{m}$  on a freezing microtome. Sections through crus IIa were cut either parasagittally or transversely. Sections through the pons were cut transversally and sections through SI frontally. (The transverse plane is here defined as a plane perpendicular to the axis through the descending fibre tract, *i.e.* the corticobulbar and corticospinal fibers, referred to as the peduncle, in the rat brainstem.) Complete series of sections from the pons, and every second section from crus IIa and SI were processed, mounted, and submitted to further analysis.

In the WGA-HRP-injected cases, sections were treated with tetramethylbenzidine (TMB) according to Mesulam (1982). Sections from the BDA-injected cases were processed according to steps 1–7 in Lanciego & Wouterlood (1994). In Pha-I-injected cases, sections were processed as outlined by Gerfen & Sawchenko (1984). For both Pha-I and BDA processing, the avidin-biotin solution used in the original protocols was substituted with the streptavidin-biotinylated horseradish-peroxidase complex (Amersham International, Buckinghamshire, UK), as employed by Lehre *et al.* (1995).

### Data acquisition

The distribution of anterogradely labelled axons and/or retrogradely labelled cell bodies was recorded through a 20 $\times$  lens using image combining computerized microscopy systems based on Leica DMR or Zeiss Axioskop 2 light and fluorescence microscopes, running the software MicroTrace (Leergaard & Bjaalie, 1995) or NeuroLucida (MicroBrightField, Colchester, VT, USA). For the animals injected with fluorescent tracers, labelling was identified using excitation light of 340–380 nm for FG and 515–560 nm for FR. The retrogradely-labelled cell bodies were coded as points, with one point corresponding to the location of each cell body (see also Brevik *et al.*, 2001; Lillehaug *et al.*, 2002). Plexuses of BDA or Pha-I labelled axons were coded semiquantitatively as points (for details, see Leergaard & Bjaalie, 1995; Leergaard *et al.*, 2000a, b). In areas with low density of labelling, points were placed at regular intervals along the length of single axons. In areas with high density of labelling, where individual fibers could not be identified, a rough correspondence was sought between the density of labelling and the number of digitized points, resulting in tight point clusters corresponding to dense axonal clusters. Similarly, in the WGA-HRP-injected animals, the putative terminal fields were point coded with a density of point coordinates corresponding to the density of TMB granules. Finally, several anatomical landmarks, such as the boundaries of the pontine nuclei, the midline, the outlines of the fourth ventricle, and the ventral pial surface of the pons, were recorded as reference lines for alignment of the sections through the pontine nuclei during the three-dimensional reconstruction procedure (below).

### Three-dimensional reconstruction and data analysis

For 3-D visualization and analysis of the distribution of labelling, we used the programs *Micro3D* for Silicon Graphics workstations (Neural Systems and Graphics Computing Laboratory, University of Oslo, Oslo, Norway, <http://www.nesys.uio.no>, see also Leergaard & Bjaalie, 2002; Bjaalie & Leergaard, 2005, 2006; Bjaalie *et al.*, 2006) and *m3d* for computers equipped with Java 3D (<http://www.rbwb.org>, FACCs application, and [java3d.dev.java.net](http://java3d.dev.java.net)). The digitized sections were aligned interactively on the screen with the aid of the reference lines as outlined in Bjaalie & Leergaard (2006) and transferred to a standardized pontine coordinate system using affine transformation procedures (for further details, see Brevik *et al.*, 2001; Bjaalie *et al.*, 2005; Bjaalie & Leergaard, 2006). The distributions of labelled cells in

the pontine nuclei for each case are shown as dot maps in simplified diagrams derived from the pontine coordinate system, displayed as projections viewed from ventral and rostral. Data were normalized and combined in a common, standardized pontine coordinate system using affine transformation procedures. Isosurfaces enveloping point populations were generated using tools available in *m3d*. Tools available in *Micro3D* were used for subdividing reconstructions in slices. Two-dimensional density maps were produced by dividing projections of the coordinate-system containing point-data, into squares of  $5 \times 5 \mu\text{m}$ , and assigning a colour to each square corresponding to the density of point coordinates within a circle with a radius of  $50 \mu\text{m}$  centred on the square. Nearest neighbour analysis was performed by measuring the distance of each point in one dataset to its closest neighbour in another dataset using the 'Sphere' tool available in the FACCS application (<http://www.rbwb.org>; Strokkenes & Bjaalie, 2004). Illustrations were assembled with Adobe Illustrator CS and Adobe Photoshop CS. Digital microscope images were obtained through the analySIS Pro v3.1 software/hardware package with the F-View digital camera (Soft Imaging System GmbH, Münster, Germany).

### Data sharing

Data from six animals included in this study have also been submitted to an online public neuroscience database holding published data describing structure and structure-function relationships in the cerebro-cerebellar system (<http://www.rbwb.org>; Bjaalie *et al.*, 2005). This database (entitled Functional Anatomy of the Cerebro-Cerebellar system) gives access to experimental data sets from several publications as well as a suite of tools for visualization and analysis of any selected combination of data sets.

## Results

Results from 15 animals were analysed. All animals were injected in crus IIa; nine of these animals were also concurrently injected in SI. Of the crus IIa injections, two covered the entire crown of the folium whereas the remaining were restricted to smaller regions of the ipsilateral upper lip patch found in the central crown of this folium. In addition, previously published 3-D reconstruction data from two corticopontine (data from Leergaard *et al.*, 2000b) and three pontocerebellar (data from Odeh *et al.*, 2005) tracing experiments were downloaded from a public data repository (<http://www.rbwb.org>; see also Bjaalie *et al.*, 2005) and analysed in combination with the newly collected data.

### Electrophysiological micromapping of crus IIa and SI cortex

Our detailed micromapping of tactile responses in SI cortex and in the granule cell layer of crus IIa generated data in agreement with previous reports from SI (Fig. 1A; Welker, 1976; Chapin & Lin, 1984; Hoffer & Alloway, 2001) and crus IIa (Figs 1C and, 2A and B; Shambes *et al.*, 1978; Bower & Kassel, 1990; Welker, 1987). As concerns the map recorded in crus IIa, we confirmed previous findings that the central region of the crown of crus IIa is dominated by tactile representations of the ipsilateral upper lip (Fig. 2B; Bower & Kassel, 1990; Gonzalez *et al.*, 1993; Morissette & Bower, 1996). This central ipsilateral upper lip representation includes the ipsilateral upper lip itself, as well as a specialized skin region located inside the mouth referred to as the ipsilateral furry buccal pad (Fig. 2). We will here use the terminology used by Hallem *et al.* (1999) and refer to these

representations together as the centrally located ipsilateral upper lip related patch of crus IIa. Regions more medial and lateral to this upper lip related patch contain a multitude of smaller patches representing a wide range of ipsilateral (and contralateral) perioral structures, including upper lip, lower lip, lower and upper incisors as previously reported (Bower & Kassel, 1990; see also Fig. 2A).

### Injection sites

Nearly all tracer injections or tracer crystal implantations were classified according to the maximum width of tracer labelling at the level of the cerebellar granule cell layer or the cerebrocortical layer V. As distinct labelling was difficult to distinguish following injection of WGA-HRP, these injection site diameters were estimated by including the densely stained halo surrounding the site of penetration. Moreover, we distinguished between tracer deposits restricted to the grey matter and those that spread into white matter. The material provided a range of tracer deposit sizes. The locations and extents (maximum widths) of the tracer deposits were mapped onto standard diagrams for the crus IIa and SI cortex. In 13 animals, tracers were placed centrally in electrophysiologically defined locations. Small and medium sized injections targeted to the centre of the large central upper lip related patch of crus IIa ranged in diameter from 150 to 600  $\mu\text{m}$ , and were most likely well confined within the boundaries of this patch, which extends  $\sim 800 \mu\text{m}$  from medial to lateral across the zebrin II-positive regions P5b+ and P6b+ (Hallem *et al.*, 1999). In two animals tracer was deposited into the central upper lip related patch of crus IIa, using (i) anatomical landmarks and vascular patterns (as registered from the electrophysiological mapping experiments) as a guidance, and (ii) histological verification of the tracer location with antizebrin staining (Hallem *et al.*, 1999; Brevik *et al.*, 2001). The tracer implantation sites were in both cases found to be located within the zebrin II-positive region P5b+, which previously has been demonstrated to be inside the spatial domain of this upper lip related patch at the crown of crus IIa (Hallem *et al.*, 1999).

### Distribution of pontine nuclei cells projecting to crus IIa

Two different approaches were taken to study the pontine projections to the folium: (i) tracer injections were restricted to remain within the central upper lip related patch (13 animals), and (ii) multiple tracer injections were made to cover numerous perioral patches distributed across the crown of crus IIa (two animals).

Pontine neurons, labelled after a restricted injection into the central upper lip related patch at the crown of crus IIa mainly occupied the central aspect of the contralateral pontine nuclei. Of the 13 animals injected in this way, 9 were submitted to an analysis of the distribution of cells on both sides of the pontine nuclei (the remaining four were only mapped contralateral to the injection site). In these 9 animals,  $97 \pm 1\%$  (mean  $\pm$  SEM) of the labelled neurons were located in the contralateral pontine nuclei, with a range of 93–100% (see also Figs 3 and 4A–C). As the pontine nuclei receive primarily somatosensory input from the ipsilateral SI cortex (holding contralateral somatosensory body part representations), the present anatomical observation provides a substrate for the strong predominance of ipsilateral body part responses in this patch (Shambes *et al.*, 1978; Bower *et al.*, 1981; Bower & Kassel, 1990).

We also found that the distribution of labelled pontocerebellar neurons varied with the size and depth of the tracer injections. When the injection sites covered a large part of the central upper lip related patch of crus IIa (injection site diameter 200–450  $\mu\text{m}$ ), the ensuing (extensive) labelling patterns were highly reproducible, even with the

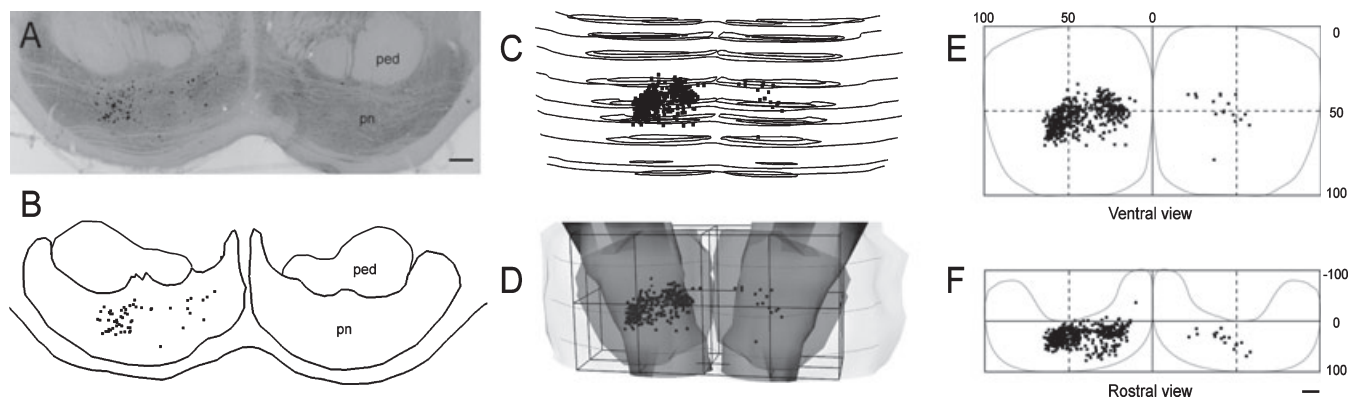


FIG. 3. Data acquisition, 3-D reconstruction and simplified presentation diagrams. (A) Composite image of a transverse section through the pontine nuclei, viewed from rostral, showing the distribution of ponto-cerebellar neurons labelled after injection of Fluoro-Ruby into the central upper lip related patch in the left crus IIa. The image was captured through a fluorescence microscope and subsequently inverted to facilitate presentation. (B) Computerized plot of the section shown in A. Each labelled neuron is represented by a dot. Lines indicate the boundaries of the pontine nuclei, the descending peduncles, and the brain stem surface. (C) Series of digitized transverse sections are registered according to anatomical landmarks, viewed from ventral. Dots, representing labelled neurons, are randomly distributed within the 50  $\mu\text{m}$  thickness of each serial section. In D, the outer boundaries of the brain stem and pontine nuclei are shown as transparent surfaces, and the boundaries of the peduncles as solid surfaces. A bounding box, representing our standard coordinate system for the pontine nuclei, has been orientated along the long axis of the brain stem and fitted to the external boundaries of the pontine nuclei. (E and F) Simplified presentation diagrams showing the distribution of labelled objects as dots in relation to the standard pontine coordinate system, shown as projections in views from ventral and rostral. Scale bars, 200  $\mu\text{m}$ .

use of different tracers (FR, BDA, FG). For these injections, the spatial extent of the clusters of labelled cells clearly correlated with the measured diameter of the injection site (Fig. 5D'–F'). The labelled neurons were typically distributed in one or two loose clusters within the contralateral pontine nuclei (Figs 3, 4A and B, and 5D'–F'), confined to a central core region ventral to the descending corticobulbar and corticospinal tract (peduncle). In the ipsilateral pontine nuclei, lower numbers of labelled neurons were found, typically located in regions mirroring those containing the contralateral labelling (Figs 3E and F, and 4A and B). In two of the cases illustrated (Fig. 4A and B), the labelled cells were distributed within volumes of similar size ( $\sim 0.07 \text{ mm}^3$  and  $\sim 0.09 \text{ mm}^3$ , respectively) at relatively similar density levels (1753 and 2713 cells/ $\text{mm}^3$ ). By contrast, following a smaller BDA injection (diameter 150  $\mu\text{m}$ ) that covered a considerably smaller part of the central upper lip related patch, labelled cells had a more restricted distribution (Figs 4C and 5D'). In this case, the volume of the pontine nuclei containing labelled cells was only  $\sim 0.02 \text{ mm}^3$ , while the density of labelled cells within this restricted subregion was at approximately the same level (2146 cells/ $\text{mm}^3$ ) as in the cases with larger injections. A similarly restricted labelling pattern was observed following a somewhat larger injection of WGA-HRP (diameter 450  $\mu\text{m}$ ), probably as a consequence of a more limited zone of tracer uptake as compared to BDA. This notion is supported by previous reports that the halo of staining typically surrounding the 'effective' WGA-HRP injection site (by necessity included in our estimate of injection site diameter, see above), does not give rise to detectable labelling (Apps, 1990; Köbbert *et al.*, 2000). The latter observations may be taken to support the presence of a within-patch topographic organization (Shambes *et al.*, 1978; Bower *et al.*, 1981; Bower & Kassel, 1990).

In the two experiments with multiple tracer injections placed across the entire crown of crus IIa, labelled neurons were found in the same central region of the contralateral pontine nuclei as described above, however, with a somewhat more extensive distribution. In the case illustrated (Fig. 4D), labelled cells were distributed within a volume of  $\sim 0.11 \text{ mm}^3$  with a density of 6680 cells/ $\text{mm}^3$ . Compared to the cases that were injected into the central upper lip patch only, the volume of labelling was only 20–40% higher but the density of labelled cells was approximately three times higher. Tracer injections into the deeper

regions of crus IIa give rise to similar distribution patterns (A. Brevik, T.B. Leergaard, E. De Schutter, & J.G. Bjaalie, unpublished results), indicating that also the deeper regions of crus IIa receive input from the central region of the contralateral pontine nuclei.

The overall similarity in spatial distribution of labelled cells following tracer injection restricted to one upper lip patch and multiple tracer injections covering a large part of the entire folium (presumably including many patches, including for example lower lip, upper and lower incisor representations, Fig. 1C) might at first seem surprising. However, analysis of the ratio of upper lip related patches in crus IIa to those representing other perioral surfaces shows that 69% of the folium actually represents the ipsilateral upper lip (Shumway *et al.*, 1999). Accordingly, tracer injections covering multiple patches at the crown of crus IIa would necessarily include some nonupper lip patches, but predominantly additional upper lip related patches. As shown in Fig. 4, the most conspicuous difference between the two groups of experiments is found in the increased density of contralaterally labelled cells, and the increased number of labelled cells in the ipsilateral pontine nuclei (Fig. 4). In the experiment illustrated in Fig. 4D, 17% of the labelled cells were found in the ipsilateral pontine nuclei, in contrast to on average 3% ipsilateral labelling found after single injections into the central upper lip related patch (Figs 3 and 4A–C, see above). This finding almost certainly reflects that the large injection sites included contralateral and bilateral upper lip representations found in the medial part of crus IIa (Fig. 2B, Bower & Kassel, 1990).

With the aim of mapping the correspondence between the cerebropontine and pontocerebellar projections, dual-labelling experiments were conducted in which an injection into the central upper lip patch of crus IIa was accompanied by an injection into the corresponding body representation of SI in the same animal. The results from nine such experiments showed that the anterogradely labelled clusters of SI projections were well defined, spherical of shape, and located centrally in the pontine nuclei in essentially the same location as the cells retrogradely labelled following tracer injections in crus IIa. (three cases illustrated in Fig. 5). Within this restricted region, high resolution analysis of the labelling patterns revealed a high degree of spatial association of labelled cells and axons, as seen in both the overview illustrations (view of the pontine nuclei from ventral,

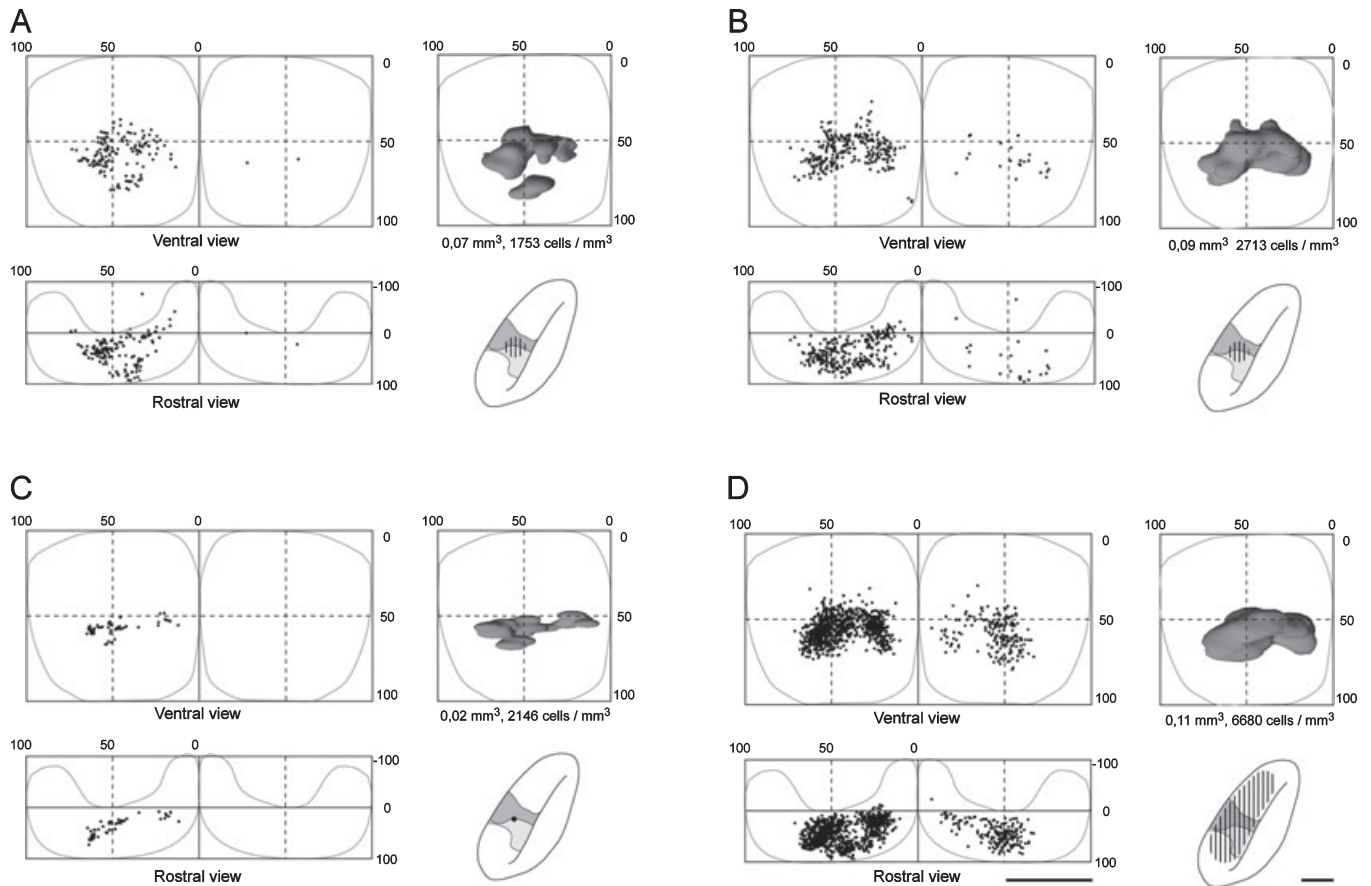


FIG. 4. Spatial distribution of pontine neurons projecting to the left cerebellar crus IIa. Computer generated dot maps and isodensity surfaces showing the distribution of ponto-cerebellar neurons labelled after restricted injection of axonal tracers into the central upper related patch in crus IIa (A–C) and multiple tracer injections into the crown of crus IIa (D) as projections viewed from ventral and rostral. Labelled neurons are shown as dots distributed within a reference frame representing our standard coordinate system for the pontine nuclei or represented by isodensity surfaces enveloping the majority of labelled cells located in the right pontine nuclei. Position within the coordinate system, relative to the intersection of the brain midline and the centre-plane of the bounding box, is given by relative coordinates from 0 to 100%. The halfway (50%) reference lines are indicated by dotted lines. The projected outlines of the pontine nuclei are shown as thin grey lines. The size and position of the injection sites is indicated by hatched areas in the drawings of crus IIa. (A and B) Tracer injection into the central upper lip related patch in crus IIa labelled delineated groups of neurons centrally in the pontine nuclei contralateral to the injection site, as well as a few ipsilaterally located neurons. (C) More restricted tracer injections in the same patch labelled clearly smaller groups of neurons in the same region. (D) Multiple tracer injections into the entire crown of crus IIa labelled considerably higher numbers of pontine neurons distributed with a higher density within a somewhat larger region, primarily in the contralateral pontine nuclei, but also ipsilaterally. (A–D) The unilateral diagrams show isodensity surfaces enveloping ~90% of the labelled cells contralaterally to the injection side (right pontine nuclei). Density of cells and the volume they occupy vary with the size of the cerebellar injection sites. Scale bars, 1 mm.

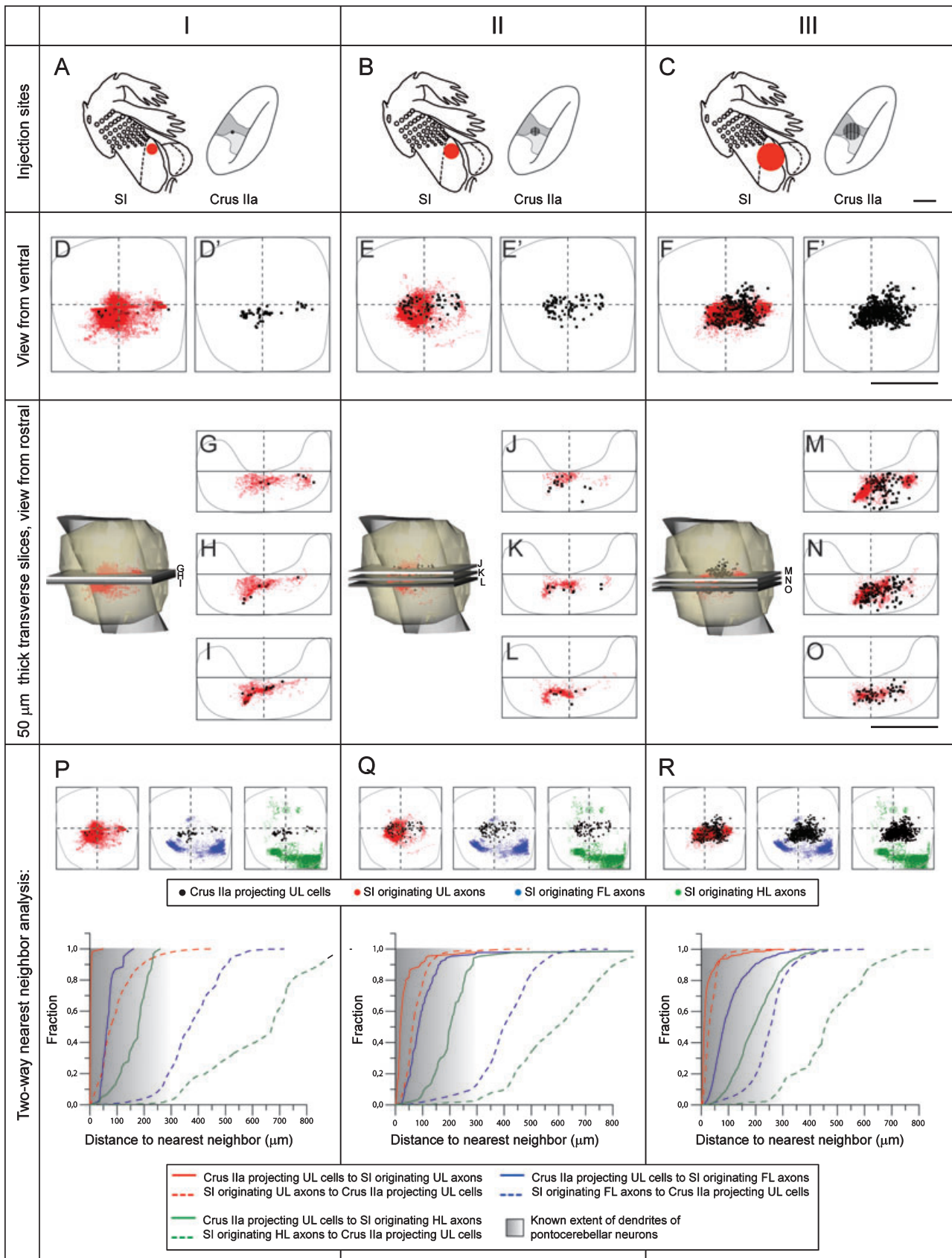
Fig. 5D–F) as well as in individual transverse slice through the reconstructions (Fig. 5G–O).

To obtain a quantitative measurement of the spatial relationship between the labelled axons and cells, we measured the distance from each crus IIa upper lip related cell to the nearest point representing an axon originating in the SI upper lip representation. This analysis revealed that 87–100% of the cells were located less than 50  $\mu\text{m}$  from

the nearest axon, and 92–100% of the cells less than 100  $\mu\text{m}$  (Fig. 5P–R, solid red curves), indicating a strong spatial association between the cells and the axons. For additional comparison, we inspected two datasets from a previous study (Leergaard *et al.*, 2000b) containing the distribution of anterogradely labelled clusters of projections originating in forelimb and hindlimb representations of SI, respectively (data downloaded from the FACCS application, <http://www.rbwb.org>). The

FIG. 5. Pontine nuclei labelling patterns in three animals that have received dual tracer injections into corresponding tactile representations in SI and crus IIa. (A–C) The filled (red and hatched) circles indicate the location and size of the respective injection sites (SI upper lip representation in the right hemisphere and ipsilateral central upper lip representation in the left crus IIa). Computer generated 3-D reconstructions of the pontine labelling are shown in view from ventral (D–F) and as 50- $\mu\text{m}$  thick transverse slices (G–O) from levels indicated in the inset 3-D reconstructions. Anterogradely labelled cerebro-pontine axons are represented by semitransparent red dots, and retrogradely labelled ponto-cerebellar neurons as black dots. Presentation is otherwise as in Fig. 3. The spatial distributions of upper lip related cerebro-pontine fibers and ponto-cerebellar neurons are overall similar. The extent of the distribution of labelled neurons (D'–F') correlates with size the tracer injection sites in crus IIa (A–C). (P–R) Graphs showing distances from each of the crus IIa projecting upper lip related cell to the nearest point representing labelled cerebro-pontine SI upper lip related axons in the 3-D reconstruction (solid red curve), as well as similar measurements of the distances separating the crus IIa projecting upper lip related cells from points representing SI forelimb (solid blue curves) or hindlimb (solid green curves) axons. The reverse measurements (from axons to cells) are shown as dashed lines. The measurements indicate a strong spatial association between the two upper lip related populations, and progressively weaker associations between the crus IIa projecting cells and axons originating from SI forelimb and hindlimb representations. The shaded grey areas indicate the approximate extent (50–300  $\mu\text{m}$ ) of dendrites of pontocerebellar neuron as estimated from previous reports (Mihailoff *et al.*, 1981; Schwarz & Thier, 1995). FL, forelimb; HL, hindlimb; SI, primary somatosensory cortex; UL, upper lip. Scale bars, 1 mm.

Dual tracer injections in corresponding tactile representations in SI and Crus IIa



comparison is shown in Fig. 5P–R. These measurements showed that the distances were progressively larger from crus IIa cells to SI upper lip axons, SI forelimb axons, and SI hindlimb axons (Fig. 5P–R, compare red, blue and green solid curves). To further identify properties in the distributions not revealed with this analyses, we also performed a reverse measurement, i.e. from the axons to the nearest cells. The reversed measurements for each pair revealed that the majority of the forelimb and hindlimb axons were distributed more than 200–300  $\mu\text{m}$  from the labelled cells, whereas all or almost all of the upper lip axons were distributed within 100  $\mu\text{m}$  (Fig. 5Q and R) or 200  $\mu\text{m}$  (Fig. 5P) from the nearest cell. More precisely, 68–98% of the axons were located less than 100  $\mu\text{m}$  from the nearest cell (Fig. 5P–R, dotted red lines). These distances are certainly within the range of the dendritic fields of pontocerebellar projection neurons (see Discussion). The most striking variation between cases is seen in the measurement of nearest neighbour distance from SI upper lip axons to crus IIa projecting cells (Fig. 5P–R, dashed red curves). In case I (Fig. 5P, same case as shown in Fig. 4C), the dashed curve is skewed to the right in comparison with the other cases. This reflects the fact that the labelled cells in this case (probably due to a smaller tracer injection site) are distributed within a smaller subvolume of the pontine nuclei than the cells and axons in the other cases.

Finally, in order to quantify our overall impression that the corticopontine and pontocerebellar components of the cerebro-cerebellar system are generally in register in the pontine nuclei, we combined and compared data from two groups of experiments. Cross examination and density gradient analysis of five accumulated data sets resulting from SI upper lip injections and seven accumulated data sets resulting from crus IIa central upper lip patch injections, clearly demonstrated that the two distributions occupied similar, largely overlapping regions within the central region of the pontine nuclei. The overall spatial congruence between the two labelling patterns was evident both from the dot maps and density maps shown in Fig. 6 (left and middle column).

In conclusion, fibers originating in SI upper lip representations and cells projection to a major crus IIa upper lip patch are both located in the same central regions of the pontine nuclei. This observation suggests that an individual cerebellar patch receiving peripheral afferent projections from a given body part, receives cortico-pontocerebellar projections from cells distributed throughout the SI projection area for the same body part. As there are many patches in each cerebellar folium (and in particular in crus IIa, Fig. 1C) representing the same body part representations, it seems likely that each of these receives input from many of the same cells by way of branching of the pontocerebellar axons. The latter assumption is supported by tracings of the branching patterns of different individual cerebellar mossy fibers (Wu *et al.*, 1999).

#### *Correspondence between cells projecting to face representations in crus IIa and the paramedian lobule*

Previous physiological mapping of receptive fields in the granule cell layer of the paramedian lobule also indicated patches receiving peripheral upper lip related projections (Shambes *et al.*, 1978). However, unlike the crus IIa, the paramedian lobule (PML) overall receives more heterogeneous peripheral projections (including forelimb tactile projections, Fig. 1C). It has been demonstrated recently that pontine neurons projecting to the PML are distributed in congruence with the terminal fields of projections from functionally related regions in SI (Odeh *et al.*, 2005; Pijpers & Ruigrok, 2006). To evaluate whether pontine neurons projecting to face-related regions in different cerebellar folia are co-located, we compared the distributions

of neurons projecting to the central upper lip related patch in crus IIa (defined by mossy fibre potentials evoked by ipsilateral upper lip stimulation, present investigation) with the distribution of neurons labelled after tracer injections in parts of the PML, containing face somatosensory representations (defined by climbing fibre potentials evoked by stimulation of the contralateral face, A2-zone; Atkins & Apps, 1997; Odeh *et al.*, 2005). To this end, we downloaded three datasets (published in Odeh *et al.*, 2005) from the public database Functional Anatomy of the Cerebro-Cerebellar System (<http://www.rbwb.org>; Bjaalie *et al.*, 2005). Combined visualization of the two groups of data points demonstrated that the neurons projecting to the PML were generally located in the same central region of the pontine nuclei as the crus IIa projecting neurons, albeit with a wider rostral and caudal distribution (Figs 6 and 7). The PML data also include more bilateral pontine labelling (Fig. 7), which most likely is due to the rather medial location of the injection sites in the PML, which would be more likely to involve bilateral receptive fields (Bower *et al.*, 1981). As already discussed, our large crus IIa injections also result in more bilateral pontine labelling (Fig. 4D). In any event, the present comparison of crus IIa and PML data (Fig. 7) show that cells projecting to face-related regions in different parts of the cerebellum have an overall similar distribution. With the presently used methods, it is not possible to determine if the same cells project to these different folia.

## Discussion

In this study, we have mapped the 3-D distribution of the neurons of origin of the pontocerebellar projection to physiologically defined parts of folium crus IIa. The distributions of these neurons were in turn compared to the distribution of SI cerebropontine projections, as well as to the distribution of pontine neurons projecting to the PML. Our findings suggest that there is a precise topographical organization of pontocerebellar neurons, corresponding to the distribution of corticopontine projections originating from SI regions with similar receptive fields. Our results support previous physiological demonstration of correspondence between the tactile maps in SI and crus IIa (Bower *et al.*, 1981). The current results, however, extend beyond previous physiological findings by (i) demonstrating the anatomical substrate for this correspondence at level of the pontine nuclei, and (ii) suggesting that the map transformation from orderly somatotopic organization in SI to fractured topography in the cerebellum primarily takes place in the mossy fibre projections from the pontine nuclei to the cerebellum. As demonstrated in other precerebellar mossy fibre systems (Woolston *et al.*, 1981; Wu *et al.*, 1999; Shinoda *et al.*, 2000), the fractured tactile cerebellar maps would appear to result from extensive branching of pontocerebellar mossy fibers.

#### *Methodological issues*

Use of 3-D computerized reconstructions and a standardized local coordinate system was essential for the across animal comparisons performed in the present study. Accuracy and consistency across experiments was further ensured by electrophysiological definition of injection locations. The across-case comparisons of accumulated data were also confirmed by dual tracer experiments conducted in the same animals. Our results clearly show that the overall distribution of pontocerebellar projections to the central upper lip related patch of crus IIa and upper lip related cerebropontine projections are highly reproducible, even with use of different axonal tracers (see also, Leergaard *et al.*, 2000b). The variations in distribution of labelling observed among different experiments clearly correlated with varia-

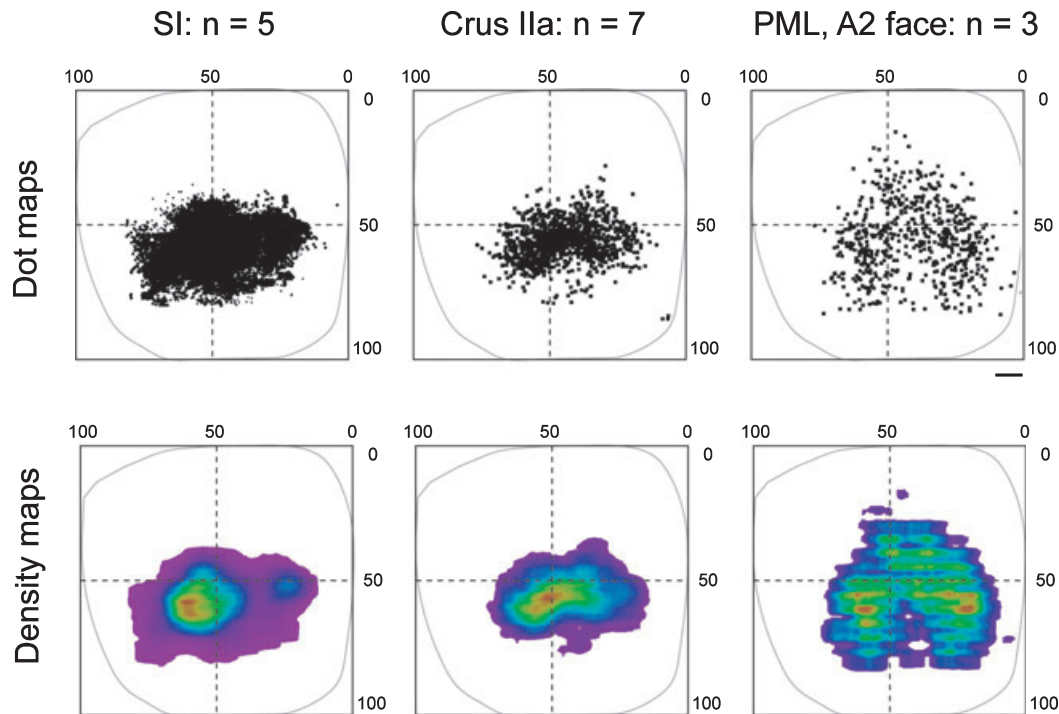


FIG. 6. Accumulated data comparison of SI-perioral cerebro-pontine projections and crus IIa projecting ponto-cerebellar neurons. Dot maps and two-dimensional density gradient maps (in view from ventral) comparing the overall distribution in the right pontine nuclei of cerebro-pontine projections arising from the upper lip representation in the right SI (left column), the central upper related patch in the left crus IIa (middle column), and the A2 face representation in the left PML (right column). Data from multiple tracing experiments were accumulated in our standard pontine coordinate system. The dot maps show that both cerebro-pontine fibers and ponto-cerebellar fibers are located in central regions of the pontine nuclei. The labelled axonal clusters appear to be more sharply defined than the aggregates of labelled ponto-cerebellar neurons, and neurons projecting to the central upper lip representation in crus IIa are more sharply defined than neurons projecting to the A2 face representation in the PML. Density gradient analysis shows that the highest relative densities (red and yellow) of both cerebro-pontine axons and ponto-cerebellar neurons are largely co-located in the pontine nuclei. Scale bar, 200  $\mu\text{m}$ .

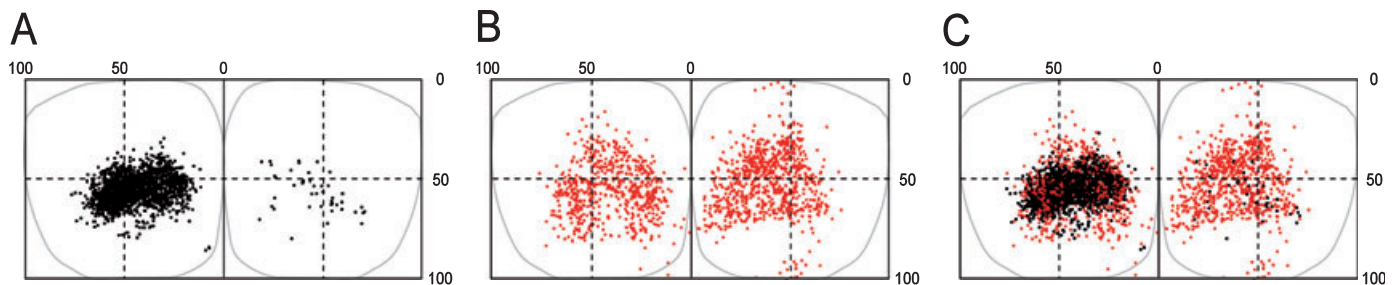


FIG. 7. Dot maps showing the bilateral distribution of upper lip/face related ponto-cerebellar cells projecting to crus IIa (A) and PML (B), respectively. Data are accumulated from multiple cases (same experiments as shown in Fig. 7), crus IIa data from the present investigation ( $n = 7$ ) and PML data from Odeh *et al.* (2005). Presentation as in Fig. 3. The two groups of points are shown together in (C). The comparison clearly shows that the central upper lip representations at the crown of crus IIa primarily receives projections from the contralateral pontine nuclei, whereas the face receiving regions of the PML receive projections from pontine with equally strong distributions in the left and right pontine nuclei. Scale bar, 200  $\mu\text{m}$ .

tions in the size of the applied tracer injections. Comparisons across experiments were facilitated by the use of a database application built on a standardized spatial reference system. The present study also demonstrates the advantage of a neuroinformatics approach allowing re-use of previously published data (Bjaalie, 2002; Bjaalie *et al.*, 2005).

#### General spatial correspondence in SI-ponto-cerebellar pathways

Taken together, various recently published anatomical data (Leergaard *et al.*, 2000b, 2004; Odeh *et al.*, 2005; Pijpers & Ruijgrok, 2006) and the present results from crus IIa, contribute to an increased under-

standing of the organization of the pathways from SI cortex onto the cerebellum. A primary finding in our study is the relatively wide distribution of the cells of origin projecting to only one of the many body representations present in the cerebellum for the upper lip. This well-defined region, located centrally in the pontine nuclei, has now been identified on basis of: (i) cerebro-pontine projections from (mossy fibre-defined) ipsilateral SI face/upper lip regions (Leergaard *et al.*, 2000b); (ii) bilateral pontocerebellar projections to the entire crown of crus IIa; (iii) mainly contralateral projections to the central upper lip related representation of crus IIa, and (iv) pontocerebellar projections to (climbing fibre-defined) face representations in the PML and crus IIb (Odeh *et al.*, 2005; Pijpers & Ruijgrok, 2006). Thus, overall the pontine cells projecting to the numerous upper lip and/or

face related representations in crus IIa, crus IIb, and the PML are distributed throughout the same volume of the pontine nuclei that receives projections from the SI upper lip area. This finding implicates that different cerebellar patches (holding similar somatosensory representations) receive projections from cells located in the same region of the pontine nuclei, and possibly also from the same cells. Mappings of individual mossy fibre trajectories in other precerebellar mossy fibre systems (Wu *et al.*, 1999) are compatible with this interpretation. Further detailed studies of pontocerebellar neuronal trajectories will be required to settle this issue. An interesting additional issue that remains unresolved is the apparent inconsistency in the maps of heterogeneous tactile representations in the granule cell layer of the PML (Fig. 1C; Shambes *et al.* 1978; Bower *et al.*, 1981) and the climbing fibre defined face-related representations recorded from the same region of the PML (Atkins & Apps, 1997; Odeh *et al.*, 2005). In this context, it is interesting to note that the pontocerebellar neurons projecting to this region of the PML appear to have a slightly more extensive distribution (potentially reflecting the heterogeneous tactile representations of the granule cell layer), as compared to neurons projecting to crus IIa (Fig. 7). It has further been reported that pontocerebellar projections are either ipsilateral or contralateral, in as much as, that pontocerebellar fibers do not seem to cross the midline within the cerebellum (Serapide *et al.*, 2002). This would imply that the population of cells giving rise to bilateral projections to the PML (Odeh *et al.*, 2005; Pijpers & Ruigrok, 2006), crus IIb (Pijpers & Ruigrok, 2006), and crus IIa (present report) consist of intermingled neurons projecting either ipsilaterally or contralaterally.

#### *From somatotopic to fractured maps*

One of the primary motivations for the present investigation was to understand the spatial transformation of tactile maps from the SI cerebral cortex to the cerebellum. While previous physiological studies demonstrated a spatial registration among ascending sensory and SI-related tactile projections to the cerebellum (Bower *et al.*, 1981), these results did not elucidate the anatomical substrate underlying the transformation from the SI somatotopic map to the fractured maps in the cerebellum. The present anatomical data strongly suggest that this map reorganization primarily occurs in the pontocerebellar pathway.

Our previous anatomical investigations have shown that the overall somatotopic organization of the SI map is preserved in a 3-D clustered map in the pontine nuclei (reviewed in Leergaard, 2003). Although cerebropontine projections typically terminate in multiple locations (clusters), the neighbouring relationships among these clusters remain preserved both at the level of major body parts (Leergaard *et al.*, 2000b), as well as among individual whisker representations (Leergaard *et al.*, 2000a, 2004). While the 3-D clustered nature of the pontine map does allow some new neighbouring relationships to be introduced, the presence of (somatotopically organized) clusters at multiple locations rather reflects a map replication than map reorganization. In the case of upper lip related SI-pontine projections, these typically terminate in two centrally located clusters (Figs 5 and 6). The current results demonstrate that retrogradely labelled cells giving rise to mossy fibre projections to crus IIa, and PML are in register with these upper lip related SI-pontine projections. Moreover, comparison of experiments in which tracer injections involved small (one upper lip related patch) or large (several perioral patches) parts of the crus IIa showed that the spatial extent of the pontine volume containing retrogradely labelled cells did not change substantially with the number of patches included in the injection site. This strongly implies that the many

different upper lip related patches at the surfaces of crus IIa receive projections from cells located within the same volume of the pontine nuclei, and thus also that the patchy and fractured organization found in the cerebellar granule cell layer results from mossy fibre branching. The current experiments do not allow us to determine whether the same pontine cells branch to project to different patches. Physiological antidromic collision tests investigating the branching structure of trigeminocerebellar mossy fibre projections have clearly shown that the same trigeminal neurons project to multiple cerebellar patches even among different folia (Woolston *et al.*, 1981). Similar anatomical data have been provided for cerebellar mossy fibre projections arising from the lateral reticular nucleus (Wu *et al.*, 1999). The present data would indicate that this is also the case for pontocerebellar projections. The fact that the general spatial location of retrogradely labelled pontocerebellar neurons is the same whether injections are made in the ipsilateral upper lip representation in crus IIa, or in regions of crus IIb and the PML, which also contain ipsilateral upper lip representations (Shambes *et al.*, 1978), suggests that the pontocerebellar mossy fibers, like those originating in the trigeminal system, also branch between folia.

#### *The finer structure of cortico-ponto-cerebellar projections*

The results presented here demonstrate that there is a high degree of spatial registration between cerebropontine and pontocerebellar projections serving the same region of the body surface. Although, fine scale spatial analysis within this region of overlap reveals that this correspondence at some points in our results is not exact, quantitative analysis showed that the large majority of SI-pontine boutons occur within 100 µm of the cell bodies of neurons generating the pontocerebellar projection. By contrast, cerebropontine projections arising from SI forelimb and hindlimb representations were predominantly located at distances exceeding 200–300 µm from upper lip related crus IIa projecting cells. Judging from Golgi stained cells (Mihailoff *et al.*, 1981) and cells visualized by intracellular fills (Schwarz & Thier, 1995), the dendrites of pontocerebellar neurons extend between 50 and 300 µm from the soma. Moreover, it is well known that synaptic boutons are predominant on distal dendrites in these cells (Holländer *et al.*, 1968; Mihailoff & McArdle, 1981). Given then, that cerebropontine terminal fields typically have a spatial extent of 50–200 µm and also display partial overlap (Leergaard *et al.*, 2000b, 2004), a substrate would seem to exist for the processing of SI information projecting through the pontine nuclei. For example, the shape and clustered distribution of cerebropontine afferents appears to introduce a further potential for spatial overlap and integration of projections from remote locations (Leergaard *et al.*, 2000b; Leergaard, 2003). Little, however, is known about the physiological properties of these neurons.

Comparisons of the distribution of pontine neurons labelled following larger and smaller injections within the central upper lip patch suggest the presence of topographical organization in the pontine nuclei, possibly reflecting an anatomical substrate for the electrophysiologically defined somatotopic organization found within patches in the granule cell layer of crus IIa (Shambes *et al.*, 1978; Bower *et al.*, 1981). A correspondingly fine SI-pontine topography can also be inferred from a previous experiment, in which a small WGA-HRP injection (assumed to have only a limited zone of tracer uptake at the injection site; Apps, 1990; Köbber *et al.*, 2000) into the SI upper lip representation gave rise to pontine labelling with more restricted distribution than expected from experiments using different tracers (<http://www.nesys.uio.no/Database>, case R105 from Leergaard *et al.*, 2000b; see also <http://www.rbwb.org>). These findings are

compatible with reports of discontinuous distributions of pontocerebellar mossy fibers (Serapide *et al.*, 2001; Voogd *et al.*, 2003), but do not elucidate further the organization of mossy fibre terminals in the cerebellar cortex. The presence and significance of such fine-scaled topographical arrangements in the cerebro-ponto-cerebellar system will require further investigations.

### Functional implications

More detailed structural and physiological information on pontocerebellar neurons are needed before we can start to understand any role of the pontine nuclei other than a means to transform one type of spatial representation (somatotopic) into another (fractured). However, the anatomical data presented here do suggest that multiple locations in the cerebellum may receive similar information through this map transformation. It has previously been established that remote cerebellar patches representing the same tactile surface receive similar peripheral (trigemino-cerebellar) input, as mossy fibers from individual trigeminal neurons target different patches, even across cerebellar folia (Woolston *et al.*, 1981). As outlined above, a similar organization is likely to be present in pontocerebellar pathways, although additional experiments are needed to make this certain. If however, information pertaining to the same tactile surfaces are distributed to different regions of the cerebellum by way of trigemino-cerebellar, as well as pontocerebellar pathways, and that information, once it arrives in the granule cell layer is processed through a similar cerebellar cortical network, then it is likely that region-dependent differences in the cerebellar processing is determined by the organization of the afferent (precerebellar) maps. It has been pointed out previously (Bower & Kassel, 1990; Bower *et al.*, 2002) that such a circumstance would require any computational theory of cerebellar function to take into account the detailed structure of the afferent maps. As shown here, these maps are generated by an equally detailed and fine anatomical structure in projecting networks.

### Acknowledgements

We thank Christian Pettersen and Anna Torbjørg Bore for expert technical assistance, and John Thompson, Kjersti Lyngstad, Antonia Volny-Luragi, and Asgeir Brevik for valuable contributions to the experimental work at an early stage. This project was funded by an EC grant QLG3-CT 2001-002256 to JGB and EDS, FWO to EDS, National Institutes of Health Grant NS-22205 to JMB, and The Research Council of Norway.

### Abbreviations

3-D, three dimensional; BDA, biotinylated dextran amine; FG, fluoro-gold; FR, rhodamine conjugated dextran amine; SI, primary somatosensory cortex; Pha-I, *Phaseolus vulgaris*-leucoagglutinin; PML, paramedian lobule; WGA-HRP, wheat germ agglutinin-horseradish peroxidase.

### References

Apps, R. (1990) Columnar organisation of the inferior olive projection to the posterior lobe of the rat cerebellum. *J. Comp. Neurol.*, **302**, 236–254.  
 Atkins, M.J. & Apps, R. (1997) Somatotopic organization within the climbing fibre projection to the paramedian lobule and copula pyramidis of the rat cerebellum. *J. Comp. Neurol.*, **389**, 249–263.  
 Bjaalie, J.G. (2002) Localization in the brain: new solutions emerging. *Nature Neurosci. Rev.*, **3**, 322–325.  
 Bjaalie, J.G. & Leergaard, T.B. (2005) Three-dimensional visualization and analysis of wiring patterns in the brain: Experiments, tools, models and databases. In Koslow, S.H. & Subramaniam, S., (Eds), *Databasing the Brain*. Wiley, Hoboken, NJ, pp. 350–368.

Bjaalie, J.G. & Leergaard, T.B. (2006) Three-dimensional computerized reconstruction from serial sections: cells populations, regions, and whole brain. In Zaborszky, L., Wouterlood, F.G. & Lanciego, J.L., (Eds), *Neuroanatomical Tract Tracing: Molecules, Neurons and Systems*. Springer Science and Business Media, New York, pp. 530–565.  
 Bjaalie, J.G., Leergaard, T.B., Lillehaug, S., Odeh, F., Moene, I.A., Kjode, J.O. & Darin, D. (2005) Database and tools for analysis of topographic organization and map transformations in major projection systems of the brain. *Neuroscience*, **136**, 681–695.  
 Bjaalie, J.G., Pettersen, C. & Leergaard, T.B. (2006) Micro3D: computer program for three-dimensional reconstruction, visualization and analysis of neuronal populations and brain regions. *Int. J. Neurosci.*, **116**, 515–540.  
 Bower, J.M. (2002) The functional organization of cerebellar circuitry reconsidered. In Highstein, S.M., & Thach, T.W., (Eds), *The Cerebellum: Recent Developments in Cerebellar Research*, Ann. N.Y. Acad. Sci. Vol. 978, New York, pp. 135–155.  
 Bower, J.M., Beermann, D.H., Gibson, J.M., Shambes, G.M. & Welker, W. (1981) Principles of organization of a cerebro-cerebellar circuit. Micromapping the projections from cerebral (SI) to cerebellar (granule cell layer) tactile areas of rats. *Brain Behav. Evol.*, **18**, 1–18.  
 Bower, J.M. & Kassel, J. (1990) Variability in tactile projection patterns to cerebellar folia crus IIA of the Norway rat. *J. Comp. Neurol.*, **302**, 768–778.  
 Brevik, A., Leergaard, T.B., Svanevik, M. & Bjaalie, J.G. (2001) Three-dimensional computerised atlas of the rat brain stem precerebellar system: approaches for mapping, visualization, and comparison of spatial distribution data. *Anat. Embryol.*, **204**, 319–332.  
 Brodal, A. (1972) Cerebrocerebellar pathways. Anatomical data and some functional implications. *Acta Neurol. Scand. Suppl.*, **51**, 153–195.  
 Chapin, J.K. & Lin, C.S. (1984) Mapping the body representation in the SI cortex of anesthetized and awake rats. *J. Comp. Neurol.*, **229**, 199–213.  
 Fabri, M. & Burton, H. (1991) Ipsilateral cortical connections of primary somatic sensory cortex in rats. *J. Comp. Neurol.*, **311**, 405–424.  
 Gerfen, C.R. & Sawchenko, P.E. (1984) An anterograde neuroanatomical tracing method that shows the detailed morphology of neurons, their axons and terminals: immunohistochemical localization of an axonally transported plant lectin, *Phaseolus vulgaris* leucoagglutinin (PHA-L). *Brain Res.*, **290**, 219–238.  
 Glover, J.C. (1995) Retrograde and anterograde axonal tracing with fluorescent dextran-amines in the embryonic nervous system. *Neurosci. Prot.*, **30**, 1–13.  
 Gonzalez, L., Shumway, C., Morissette, J. & Bower, J.M. (1993) Developmental plasticity in cerebellar tactile maps: fractured maps retain a fractured organization. *J. Comp. Neurol.*, **332**, 487–498.  
 Hallem, J.S., Thompson, J.H., Gundappa-Sulur, G., Hawkes, R., Bjaalie, J.G. & Bower, J.M. (1999) Spatial correspondence between tactile projection patterns and the distribution of the antigenic Purkinje cell markers anti-zebrin I and anti-zebrin II in the cerebellar folium crus IIA of the rat. *Neuroscience*, **93**, 1083–1094.  
 Hartmann, M.J. & Bower, J.M. (2001) Tactile responses in the granule cell layer of cerebellar folium crus IIA of freely behaving rats. *J. Neurosci.*, **21**, 3549–3563.  
 Hawkes, R. & Leclerc, N. (1986) Immunocytochemical demonstration of topographic ordering of Purkinje cell axon terminals in the fastigial nuclei of the rat. *J. Comp. Neurol.*, **244**, 481–491.  
 Hoffer, Z.S. & Alloway, K.D. (2001) Organization of corticostriatal projections from the vibrissal representations in the primary motor and somatosensory cortical areas of rodents. *J. Comp. Neurol.*, **439**, 87–103.  
 Holländer, H., Brodal, P. & Walberg, F. (1968) Electronmicroscopic observations on the structure of the pontine nuclei and the mode of termination of the corticopontine fibres. An experimental study in the cat. *Exp. Brain Res.*, **7**, 95–110.  
 Köbbert, C., Apps, R., Bechmann, I., Lanciego, J.L., Mey, J. & Thanos, S. (2000) Current concepts in neuroanatomical tracing. *Prog. Neurobiol.*, **62**, 327–351.  
 Lanciego, J.L. & Wouterlood, F.G. (1994) Dual anterograde axonal tracing with *Phaseolus vulgaris*-leucoagglutinin (PHA-L) and biotinylated dextran amine (BDA). *Neurosci. Protocols*, **94-050-06-01-13**.  
 Leergaard, T.B. (2003) Clustered and laminar topographic patterns in rat cerebro-pontine pathways. *Anat. Embryol.*, **206**, 149–162.  
 Leergaard, T.B., Alloway, K.D., Mutic, J.J. & Bjaalie, J.G. (2000a) Three-dimensional topography of corticopontine projections from rat barrel cortex: correlations with corticostriatal organization. *J. Neurosci.*, **20**, 8474–8484.  
 Leergaard, T.B., Alloway, K.D., Pham, T.A., Bolstad, I., Hoffer, Z.S., Pettersen, C. & Bjaalie, J.G. (2004) Three-dimensional topography of corticopontine projections from rat sensorimotor cortex: comparisons with corticostriatal

- projections reveal diverse integrative organization. *J. Comp. Neurol.*, **478**, 306–322.
- Leergaard, T.B. & Bjaalie, J.G. (1995) Semi-automatic data acquisition for quantitative neuroanatomy. MicroTrace – computer programme for recording of the spatial distribution of neuronal populations. *Neurosci. Res.*, **22**, 231–243.
- Leergaard, T.B. & Bjaalie, J.G. (2002) Architecture of sensory map transformations: axonal tracing in combination with 3-D reconstruction, geometric modeling, and quantitative analyses. In Ascoli, G., (Ed), *Computational Neuroanatomy: Principles and Methods*. Humana Press, Totowa, NJ, pp. 119–217.
- Leergaard, T.B., Lyngstad, K.A., Thompson, J.H., Taeymans, S., Vos, B.P., De Schutter, E., Bower, J.M. & Bjaalie, J.G. (2000b) Rat somatosensory cerebropontocerebellar pathways: spatial relationships of the somatotopic map of the primary somatosensory cortex are preserved in a three-dimensional clustered pontine map. *J. Comp. Neurol.*, **422**, 246–266.
- Lehre, K.P., Levy, L.M., Ottersen, O.P., Storm-Mathisen, J. & Danbolt, N.C. (1995) Differential expression of two glial glutamate transporters in the rat brain: quantitative and immunocytochemical observations. *J. Neurosci.*, **15**, 1835–1853.
- Lillehaug, S., Oyan, D., Leergaard, T.B. & Bjaalie, J.G. (2002) Comparison of semi-automatic and automatic data acquisition methods for studying three-dimensional distributions of large neuronal populations and axonal plexuses. *Network*, **13**, 343–356.
- Mesulam, M.-M. (1982) Principles of horseradish peroxidase neurohistochemistry and their applications for tracing neural pathways – Axonal transport, enzyme histochemistry and light microscopic analysis. In Mesulam, M.-M., (Ed) *Tracing Neural Connections with Horseradish Peroxidase*. John Wiley & Sons, Chichester, pp. 1–151.
- Mihailoff, G.A. & McArdle, C.B. (1981) The cytoarchitecture, cytology, and synaptic organization of the basilar pontine nuclei in the rat. II. Electron microscopic studies. *J. Comp. Neurol.*, **195**, 203–219.
- Mihailoff, G.A., McArdle, C.B. & Adams, C.E. (1981) The cytoarchitecture, cytology, and synaptic organization of the basilar pontine nuclei in the rat. I. Nissl and Golgi studies. *J. Comp. Neurol.*, **195**, 181–201.
- Morissette, J. & Bower, J.M. (1996) Contribution of somatosensory cortex to responses in the rat cerebellar granule cell layer following peripheral tactile stimulation. *Exp. Brain Res.*, **109**, 240–250.
- Odeh, F., Ackerley, R., Bjaalie, J.G. & Apps, R. (2005) Pontine maps linking somatosensory and cerebellar cortices are in register with climbing fiber somatotopy. *J. Neurosci.*, **25**, 5680–5690.
- Pijpers, A. & Ruigrok, T.J.H. (2006) Organization of pontocerebellar projections to identified climbing fiber zones in the rat. *J. Comp. Neurol.*, **496**, 513–528.
- Schwarz, C. & Thier, P. (1995) Modular organization of the pontine nuclei: dendritic fields of identified pontine projection neurons in the rat respect the borders of cortical afferent fields. *J. Neurosci.*, **15**, 3475–3489.
- Serapide, M.F., Panto, M.R., Parenti, R., Zappala, A. & Cicirata, F. (2001) Multiple zonal projections of the basilar pontine nuclei to the cerebellar cortex of the rat. *J. comp. Neurol.*, **430**, 471–484.
- Serapide, M.F., Zappala, A., Parenti, R., Panto, M.R. & Cicirata, F. (2002) Laterality of the pontocerebellar projections in the rat. *Eur. J. Neurosci.*, **15**, 1551–1556.
- Shambes, G.M., Gibson, J.M. & Welker, W. (1978) Fractured somatotopy in granule cell tactile areas of rat cerebellar hemispheres revealed by micromapping. *Brain Behav. Evol.*, **15**, 94–140.
- Shinoda, Y., Sugihara, I., Wu, H.S. & Sugiuchi, Y. (2000) The entire trajectory of single climbing and mossy fibers in the cerebellar nuclei and cortex. *Prog. Brain Res.*, **124**, 173–186.
- Shumway, C.A., Morissette, J., Gruen, P. & Bower, J.M. (1999) Plasticity in cerebellar tactile maps in the adult rat. *J. Comp. Neurol.*, **413**, 583–592.
- Strokkenes, G. & Bjaalie, J.G. (2004) The ‘overlap problem’ in neuroanatomy: quantitative approaches to the study of three-dimensional distribution patterns. *FENS Abstr.*, **2**, A026.2.
- Voogd, J. (1995) Cerebellum. In Bannister, L.H., Berry, M.M., Collins, P., Dyson, M., Dussek, J.E. & Ferguson, M.W.J., (Eds), *Gray’s Anatomy*. Churchill Livingstone, New York, pp. 1027–1065.
- Voogd, J., Pardoe, J., Ruigrok, T.J. & Apps, R. (2003) The distribution of climbing and mossy fiber collateral branches from the copula pyramidis and the paramedian lobule: congruence of climbing fiber cortical zones and the pattern of zebrin banding within the rat cerebellum. *J. Neurosci.*, **23**, 4645–4656.
- Welker, C. (1971) Microelectrode delineation of fine grain somatotopic organization of (Sml) cerebral neocortex in albino rat. *Brain Res.*, **26**, 259–275.
- Welker, C. (1976) Receptive fields of barrels in the somatosensory neocortex of the rat. *J. Comp. Neurol.*, **166**, 173–189.
- Welker, W. (1987) Spatial organization of somatosensory projections to granule cell cerebellar cortex: Functional and connectional implications of fractured somatotopy (summary of Wiscounsin studies). In King, J.S., (Eds), *New Concepts in Cerebellar Neurobiology*. A.R. Liss, New York, pp. 239–280.
- Woolsey, T.A. & Van der Loos, H. (1970) The structural organization of layer IV in the somatosensory region (SI) of mouse cerebral cortex. The description of a cortical field composed of discrete cytoarchitectonic units. *Brain Res.*, **17**, 205–242.
- Woolston, D.C., Kassel, J. & Gibson, J.M. (1981) Trigemino-cerebellar mossy fiber branching to granule cell layer patches in the rat cerebellum. *Brain Res.*, **209**, 255–269.
- Wu, H.S., Sugihara, I. & Shinoda, Y. (1999) Projection patterns of single mossy fibers originating from the lateral reticular nucleus in the rat cerebellar cortex and nuclei. *J. Comp. Neurol.*, **411**, 97–118.